Finite element analysis of a rigid beam to column connection reinforced with channels

Farzaneh Ghalamzan Esfahani * Nader Fanaie**

Abstract:

   This research work presents a new rigid connection constructed with channels. In order to assess its hysteresis behavior, three specimens with different cover plates and six specimens with different panel zone thickness have been considered. The energy absorbed by the connection and the behavior of the panel zone were studied during cyclic loading and compared with those of connection specimens constructed with ribs, as presented in previous researches. Based on the performed analyses, the connection constructed with channels can withstand a rotation of 0.06 radian without considerable strength reduction. In addition, more energy was absorbed in the suggested connection compared to the connection constructed with ribs, while lower rotation was created in the panel zone. Furthermore, the results of the absorbed energy and panel zone rotation are close in both kinds of connection when different lengths of cover plates are used. .

1. Introduction

   Rigid beam to column connection in moment resisting frames are ordinarily designed according to the classic beam theory of Euler- Bernoulli. According to this theory, it is assumed that the beam flanges transfer the bending moment while the web resists shear loading. Based on past studies (Lee *et al.*, 1998 [15], 2000 [16]), the above mentioned design assumptions are not practical and the stress distribution around the connections is substantially different from the assumed pattern of the classic beam theory due to the effects of boundary conditions (Lee *et al.*, 2005 [17]). The results of finite elements studies have shown that the magnitude and direction of the main stresses in the connection region are estimated more appropriately by Truss Analogy model (Goel *et al.*, 1996 [9], 1997 [10], 2000 [11]; Goswami and Murty, 2010 [12]) compared to the classic beam theory. In this model, the bending moment and shear force are both transferred to the beam flanges by the diagonal strut in the whole connection. The connection between the beam web and the column flange is not required because the beam web does not transfer the shear force to the column (Arlekar and Murty, 2004 [3]).

   In the truss analogy model, a K form truss was used to demonstrate the forces' flow which commences from the column face. Based on these forces, a connection design which consists of cover and rib plates has been suggested (Goel *et al.*, 1996 [9]). In fact, when approaching the connection region, both normal and shear stresses are concentrated in the flanges. Shear stress reaches its minimum value around the neutral axis in the beam web (Lee *et al.*, 1998 [15]).

   Practically, the beam web is mostly emptied by shear stress. As a result, the beam flange region, designed for bending moment was over loaded (Lee *et al.*, 2000 [16]). This result explains the main reason of failure in the beam flange to column connection, similar to what happened in the Northridge earthquake (1994) (Mahin *et al.*, 2002 [18]; Miller, 1998 [19]; Tremblay *et al.*, 1995 [20]).

   Therefore, the stress near the connection region has been presented through a connection model using ribs, Fig. 1 (Arlekar and Murty, 2004 [3]). Besides, the seismic behavior of moment connections used in moment-resisting frames can be improved by adding vertical ribs to beam-to-column joints (Chen *et al.*, 2004 [4]; Chen *et al.*, 2004 [5]; Chen *et al.*, 2005 [6]).

   In this research, the cyclic behavior of such connections was assessed. A connection using channels instead of outer ribs is being proposed. The seismic behavior was studied under the loading protocol of AISC Seismic Provisions for Structural Steel Buildings (AISC, 2010 [1]), using finite element software (ABAQUS) (Hibbitt *et al.*, 2011 [13]),

* M.Sc. in Structural Engineering, Department of civil engineering,
K. N . Toosi University of Technology, Iran,
E-mail: f.ghalamzan@gmail.com
** Corresponding author, Ph.D., Department of civil engineering,
K. N . Toosi University of Technology, Iran, E-mail: fanaie@kntu.ac.ir

and compared with that constructed with ribs. The effects of cover plate length, thickness of panel zone as well as the presence of continuity plates on the seismic behavior of the connection was studied. The absorbed energy and maximum rotation created in the panel zone were also calculated. The obtained results were compared with those connections constructed with ribs. The connection constructed with channels is hereafter called channel connection and the connection constructed with ribs is hereafter called rib connection.
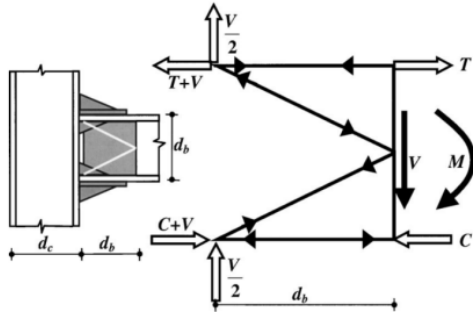

Fig. 1: The connection elements and K form truss location, forces flow in the truss analogy model near the constructed region of connection (Arlekar and Murty, 2004 [3])

2. Analytical Assessment of Channel Connection

According to the finite elements' studies, Euler Bernoulli stress distribution has no applicability around the connection region (Lee *et al.*, 2000 [16]; Goel *et al.*, 1996 [9]). The shear of the beam is deviated towards the beam flanges near the connection, which causes stress concentration in the connection point of beam flange to column flange. In this study, a form of connection which consists of cover plates, channels and inner vertical ribs have been used and is shown in Fig. 2. The presence of inner vertical ribs will reduce the potential of creating cracks in the connection point of cover plate to the column flange (Arlekar and Murty, 2004 [3]).
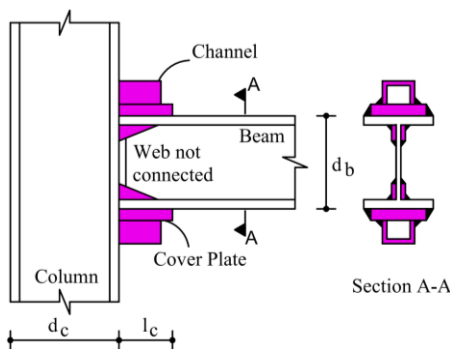

Fig. 2: The situation of the elements in channel connection

The next section will present the step by step design of the connection, assuming that the truss point is formed at a distance of half beam depth from the reinforced region of the connection (Arlekar and Murty, 2004 [3]). Finite elements analyses were conducted on the newly

constructed connection and on the rib connection. The analyses were performed to assess the nonlinear cyclic behavior and obtain moment-rotation curves of the connections, energy dissipated in the connection (the energy dissipated by plastic deformation) and maximum rotation of panel zone. The sub-assemblage considered for analysis is presented in Fig. 3. The W12×58 section is used for beam and W18×114 for column in each sub-assemblage. The specifications of these sections are presented in Table 1. The column support is hinged at both ends. The beam flanges are laterally braced at 1.8m distance from the central axis of the column. The relation presented in AISC code for seismic design is fulfilled by the mentioned distance. Fig. 3 shows the geometry and support conditions of the connections modeled in the software. In all analyses, the nonlinear behavior of steel was considered.
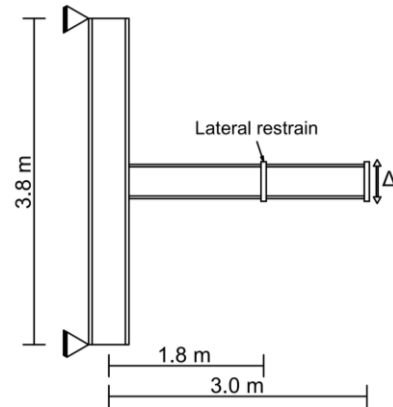

Fig. 3: Geometry and condition of supports

Table 1: The specifications of beam and column

section	h (mm)	b_f (mm)	t_f (mm)	t_w (mm)
W18×114	469	301	25	15
W12×58	310	254	16	9
Channel 80	80	45	8	6

3. Design of connections

The maximum probable moment of the beam is calculated as follows:

$$M_{pr} = C_{pr}R_yM_p \tag{1}$$

Where, $C_{pr} = (F_y + F_u)/2F_y$, R_y is the over-strength factor of FEMA 350 (FEMA 2000 [7]); $M_p = F_yZ_b$; F_y is the yielding stress; F_u is the ultimate stress; Z_b is the plastic section modulus in the location of plastic hinge formation.

It is assumed that plastic hinge is formed along the beam length at a distance of half height of the beam from the end of the constructed region of the connection. The distance between the plastic hinges (L_0) is obtained as follows:

$$L_0 = L - \left(\frac{d_c}{2} + l_c + \frac{d_b}{2} + \frac{d_b}{2} + l_c + \frac{d_c}{2}\right) \tag{2}$$

Maximum probable shear force (V_{pr}) of the connection is calculated as follows:

$$V_{pr} = 2M_{pr}/L_0 \tag{3}$$

Vertical shear force (V_d) and horizontal tension force (T_d) are computed for the upper half of the connection by Eqs. (4) and (5) respectively (Arlekar and Murty, 2004 [3]).

$$V_d = V_{pr}/2 \tag{4}$$

$$T_d = \left(M_{pr}/d_b\right) + \left(V_{pr}/2\right) \tag{5}$$

The second sentence in Eq. (5) is due to an increase in moment which is the consequence of the plastic hinge transferred from column face to the inside of beam. These forces are obtained based on the truss model in which it is assumed that the beam shear is transferred to the column by the beam flanges and not its web (Arlekar and Murty, 2004 [3]).

3.1. Design of cover plates

The weld between the beam and cover plates is subjected to the composition of shear and tension, Fig. 2. Shear and tension are calculated for this weld as follows:

$$T_{wcp} = V_d \tag{6}$$

$$V_{wcp} = T_d - T_f \tag{7}$$

Where, T_f is the capacity of beam flange, defined as $T_f = F_y b_{bf} t_{bf}$; where, b_{bf} and t_{bf} are the width and thickness of the beam flange respectively.

Eq. (8) is used to calculate the weld area needed for transferring the composed T_{wcp} and V_{wcp}.

$$A_{wcp} = \sqrt{\left(T_{wcp}^2 + 3V_{wcp}^2\right)/F_y^2} \tag{8}$$

The lengths of cover plates (l_c) were considered as half of the beam depth ($d_b/2$) (Arlekar and Murty, 2004 [3]).

3.2. Design of channels

The shear in the channel is calculated by Eq. (9), considering the connection shown in Fig. 2 and assuming that the shear is transferred to the column through the channels.

$$V_{ch} = V_d \tag{9}$$

The fillet weld between the channel and cover plates is subjected to the composed tension and shear, and calculated through Eqs. (10) and (11) respectively.

$$T_{whch} = V_{ch} \tag{10}$$

$$V_{whch} = T_{ch} = T_d - T_f - T_{cp} \tag{11}$$

Where, T_{cp} is the capacity of cover plates, defined as $T_{cp} = F_y b_{cp} t_{cp}$; where, b_{cp} and t_{cp} are the width and thickness of the cover plates respectively.

The area of fillet weld between the channel and cover plates is obtained by Eq. (12), considering the forces calculated through Eqs. (10) and (11) as follows:

$$A_{whch} = \sqrt{\left(T_{whch}^2 + 3V_{whch}^2\right)/F_y^2} \tag{12}$$

The maximum size of fillet weld between the channel and cover plates (t_{whch}) is equal to the thickness of the channel flange. The length of this weld is calculated as follows:

$$l_{whch} = A_{whch}/(t_{whch}/\sqrt{2}) \tag{13}$$

As the whole channel is connected to the cover plates with two lines of fillet weld, the channel's length is equal to the length of the obtained angle weld. The channel area which transfers the composed shear and tension to the column is obtained by Eq. (14), with respect to the forces calculated through Eqs. (9) and (11).

$$A_{ch} = \sqrt{\left(T_{ch}^2 + 3V_{ch}^2\right)/F_y^2} \tag{14}$$

The appropriate channel is used according to the obtained area. The capacities are calculated for real sizes of cover plates and channel. The connection capacity which resists external moment should be greater than the moment's demand containing the increased moment. Eq. (15) is used for this purpose as follows:

$$\left(T_{ch} + T_{cp} + T_f\right)\left(d_b + t_{cp}\right) \geq M_{pr} + V_{pr}(l_c + l_t) \tag{15}$$

The channel with the specifications presented in Table 1 is used for the considered connections. In the rib connection, the ribs have been designed like channels, except that the tension and shear forces of each rib is considered as half of the values considered for the channel. This is due to the presence of two external ribs and the connection of each rib to the column with two weld beads.

$$V_{rp} = V_d/2 \ , T_{rp} = \left(T_d - T_f - T_{cp}\right)/2 \tag{16}$$

The specifications of connection elements obtained from the design are presented in Table 2.

4. Specification of models

4.1. Changing panel zone

A weak panel zone is created by selecting W12×58 section for beam and W18×114 section for column. It attempts to evaluate the effect of the thickness of the panel zone on the seismic performance of the connection. Accordingly, the column web has been constructed with doubler plates of 8 and 15 mm thickness creating balanced and strong panel zones respectively. Three considered specimens are presented in Table 3.

The shear strength needed for the panel zone (V_r) is calculated according to FEMA 355d code (FEMA 2000 [8]) as follows:

$$V_r = \frac{\sum M_{yield-beam}}{d_b}\left(\frac{L}{L - d_c}\right)\left(\frac{h - d_b}{h}\right) \tag{17}$$

The designed shear strength (V_y) is obtained based on AISC code (AISC 2010 [2]) as follows:

$$V_y = 0.6F_{yc}d_c t_{pz}(1 + \frac{3b_{cf}t_{cf}^2}{d_b d_c t_{pz}}) \tag{18}$$

Table 2: The specifications of connection elements

Models	Cover plates			Rib plates (inner, outer)			Channel
	L (mm)	B (mm)	T (mm)	L (mm)	B (mm)	T (mm)	L (mm)
RIB	155	190	30	25	40	16	-
CH	155	190	30	25	40	16	100

Table 3: The specifications of panel zone

Specimen	Column section	Beam section	Doubler plate thickness (mm)	V_y (kN)	V_r (kN)	V_r/V_y
Weak	W18×114	W12×58	0	1328	1138	0.86
Balanced	W18×114	W12×58	8	2454	1138	0.46
Strong	W18×114	W12×58	15	3439	1138	0.33

Where, F_{yc} is yielding stress of column; d_c is column height; t_{pz} is thickness of panel zone; b_{cf} is the width of column flange; t_{cf} is the thickness of column flange; h is column height; and L is the central axis distance of the columns located at both sides of the beam. The values are presented for 3 different panel zones in Table 3.

4.2. Changing the continuity plates

Besides the thickness of the panel zone, the effect of the continuity plates on the seismic performance of the connection was assessed as well. In the models analyzed with continuity plates, the thickness of these plates were considered equal to that of cover plates (30 mm). Table 4 presents the nomination of considered models with different panel zones.

4.3. Changing the lengths of cover plates

The connection elements and cover plates have been designed using the above mentioned process. The effect of the lengths of cover plates on the seismic performance of the suggested and previous connections was assessed (Arlekar and Murty, 2004 [3]). Accordingly, three values- 50% (155 mm), 75% (230 mm) and 100% of beam height have been considered for the lengths of the cover plates. In this case, other specifications of connection elements including the thickness of cover plates as well as the sizes of rib plates and channels remain constant. The doubler plates with 8 mm thickness and continuity plates with 30 mm thickness have been used in front of the cover plates in the panel zone for all specimens (Table 5).

5. Finite Element Analysis

The ABAQUS Finite element software (Hibbitt *et al.*, 2011 [13]) was utilized to model the specimens. The main purpose of analyzing the specimens is to assess the effects of panel zone thickness, presence of continuity plates and cover

plates' lengths on the cyclic behavior of the channel sub-assemblages, amount of dissipated energy and maximum rotation of panel zone.

5.1. Material Modeling

Nonlinear material with combined hardening was used in the modeling. The plasticity model was based on the von Mises yielding criterion and its associated flow rule. Stress–strain curve of ASTM A36 steel is shown in Fig. 4. The Young's modulus of $2.1 \times 10^5\ MPa$ and Poisson's ratio of 0.3 are used as elastic constants.
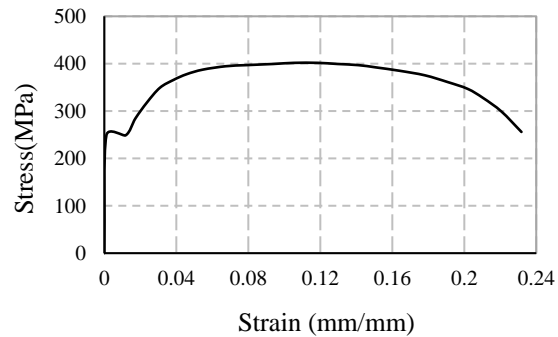
Fig. 4: Stress_strain curve of ASTM A36 steel

5.2. Elements and meshing

The four-node shell element with reduced integral (S4R) was used for the beam and the column, and the eight-node solid element with reduced integral (C3D8R) for modeling continuity plates, cover plates, ribs and channels. These elements have capability of plasticity, large deformation and large strains. Each point has three transversal degrees of freedom in addition to three rotational degrees of freedom around X, Y and Z axes. Fig. 5a shows a meshing sample for the rib connection and Fig. 5b for channel connection. A finer meshing was used for the region near the connection.

Table 4: The rib connections and channel connections along with different panel zones

Models	Continuity plate thickness(mm)	Doubler plate thickness (mm)	Models	Continuity plate thickness(mm)	Doubler plate thickness (mm)
RIBTD0	0	0	CH TD0	0	0
RIBTD0C	30	0	CH TD0C	30	0
RIBTD8	0	8	CH TD8	0	8
RIBTD8C	30	8	CH TD8C	30	8
RIBTD15	0	15	CH TD15	0	15
RIBTD15C	30	15	CH TD15C	30	15

Table 5: The models constructed with different cover plates

Models	Cover plates			Rib plates (inner, outer)			Channel
	L (mm)	B (mm)	T (mm)	L (mm)	B (mm)	T (mm)	L (mm)
RIB Cp0.5d$_b$	155	190	30	25	40	16	-
RIB Cp0.75d$_b$	230	190	30	25	40	16	-
RIB Cpd$_b$	310	190	30	25	40	16	-
CH Cp0.5db	155	190	30	25	40	16	100
CH Cp0.75d$_b$	230	190	30	25	40	16	100
CH Cpd$_b$	310	190	30	25	40	16	100

(a)

(b)
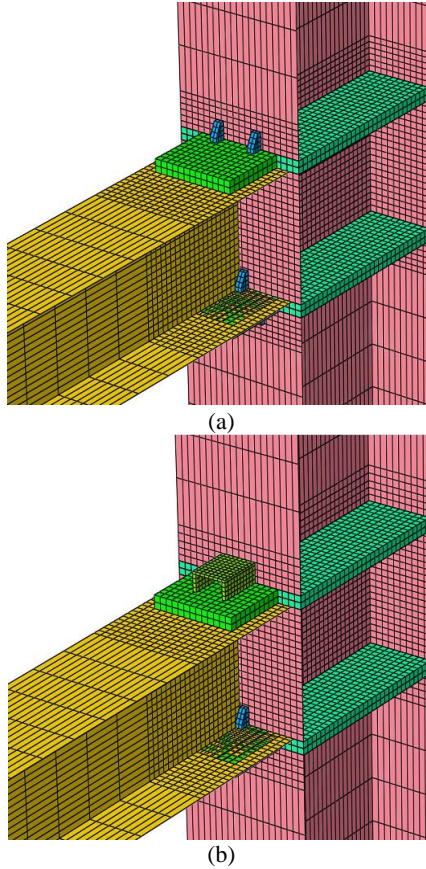
Fig. 5: Meshing the connections constructed with: a) rib; b) channel

5.3. Loading protocol

The connection models were loaded at the free end of the beam in the form of displacement control. In this regard, the loading protocol of Seismic Provisions for Structural Steel Buildings (AISC 2010 [1]) was used, presented in the form

of number of cycles in the story drift angle, θ. All specimens were loaded up to the story drift angle of 0.06 radian. The applied loading protocol is presented in Table 6.

Table 6: Loading protocol

6 cycles at θ=0.00375 rad
6 cycles at θ=0.005 rad
6 cycles at θ=0.0075 rad
4 cycles at θ=0.01 rad
2 cycles at θ=0.015 rad
2 cycles at θ=0.02 rad
2 cycles at θ=0.03 rad
2 cycles at θ=0.04 rad
2 cycles at θ=0.05 rad
2 cycles at θ=0.06 rad

6. Verification of Models

A connection sample has been modeled by Arlekar and Murty (Arlekar and Murty, 2004 [3]) using W12×58 section for beam and W18×114 for column. In order to verify the finite element models, this sample has been modeled in ABAQUS software as well. The sample was subjected to monotonic loading up to a drift of 0.07. In the relevant plotted pushover curves, the load has been normalized using plastic capacity load of beam section, shown as P$_{Pb}$and calculated as follows:

$$P_{pb} = \frac{M_{pb}}{L - (\frac{d_c}{2} + l_c)} \tag{19}$$

Where, L is the distance between the center line of the column and beam end; d_c is column depth; l_c is the length of cover plates; and M$_{Pb}$ is the plastic capacity of beam section. The drifts of connection models are defined as follows:

$$\%\text{Drift} = \frac{\Delta}{L} \times 100 \tag{20}$$

Where, Δ is the displacement of beam tip. Based on Fig. 6, the results obtained from finite element modeling are well in accordance with the pushover curve. This comparison confirms the authenticity of the results obtained from modeling in the present research.
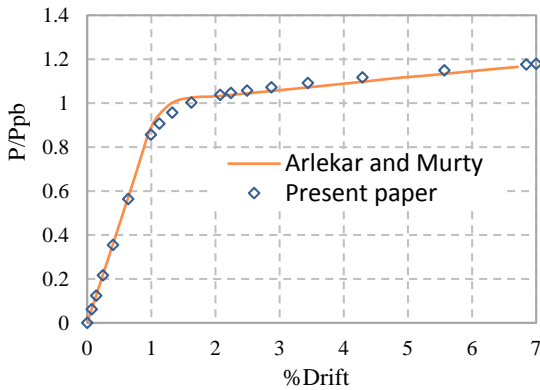

Fig. 6: Pushover curve obtained for verification

Besides, the validity of finite element model has been verified with experimental results. For this purpose, the RIB-DB30-AW specimen used in the experimental investigation of Lee *et al.* (Lee *et al.*, 2005 [14]) has been analyzed under cyclic displacement control loading by ABAQUS finite element software. The hysteresis curve and Von Mises contour of the model are presented in Figs. 7-8, respectively. In Fig. 7, the horizontal and vertical axes are drift (according to Eq. (20)) and normalized moment at column face (M/M_P), respectively; where, M_P is plastic moment of the beam at column face. Based on this figure, the results show good compatibility with the experimental findings.
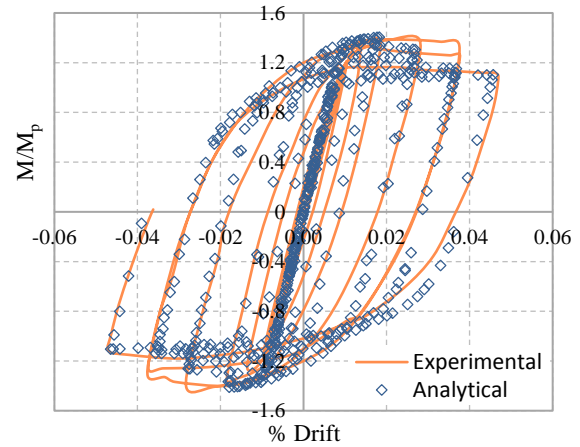
7. Results and Explanations

After verification of the considered connection concerning the designed elements in the previous sections, channel and rib connections are modeled in the software. They are analyzed under the loading protocol of AISC code by changing the lengths of cover plates and the thickness of panel zone. The results of cyclic loading obtained for the channel connection are presented in the next sections. The results of the rib connection were then compared with those of channel connection.

Fig. 7: Hysteresis curve for verifying RIB-DB30-AW model
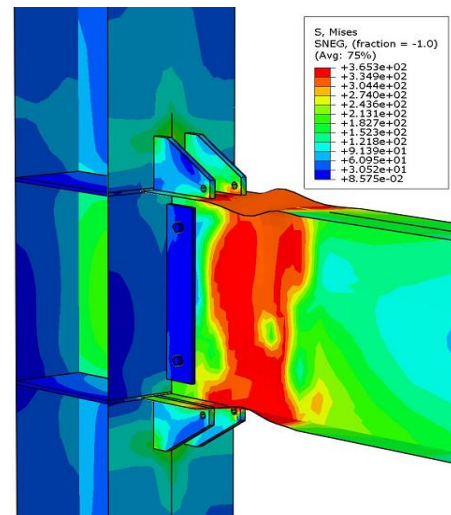
Fig. 8: Von Mises stress contour for verifying RIB-DB30-AW model

7.1. Hysteresis responses

The hysteresis moment-rotation curves have been plotted for all specimens. In this research work, only the curves of channel connection have been presented considering its similarity with that of the other connection.

The hysteresis curves of the suggested connection have been plotted by changing thickness of panel zone and adding continuity plates to the 3 panel zone cases. In these curves, the vertical axis is the moment of beam in the column face normalized, corresponding to the plastic moment of the beam section. The horizontal axis is the rotation of the beam, obtained by dividing the displacement of the beam end by the distance of the beam end from the column's central axis.
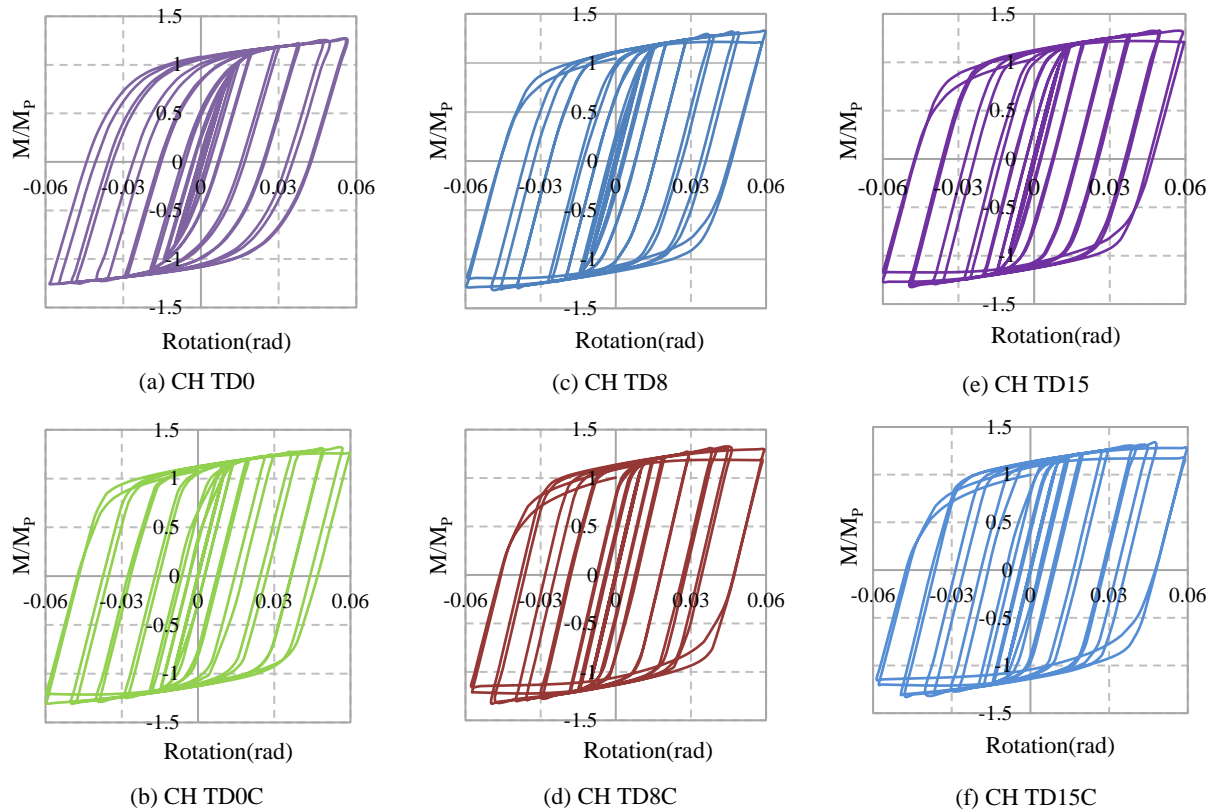
| (a) CH TD0 | (c) CH TD8 | (e) CH TD15 |
| (b) CH TD0C | (d) CH TD8C | (f) CH TD15C |

Fig. 9: Hysteresis curves of the channel connection with different panel zones

According to the Fig. 9a, the hysteresis curve is progressive in the connection without continuity and doubler plates (CH TD0). In this curve, no reduction strength is seen. Due to the high strain created in the panel zone, beam flange yielding does not occur. In this case, plastic hinge is formed inside the panel zone instead of beam. Fewer moments are obtained during the loading of this sample compared to the statuses with doubler plates and/or continuity plates. Strength reduction is observed in the hysteresis curve by adding the continuity and doubler plates to the panel zone in the final loading cycles.

As the stiffness of the panel zone is enhanced, the deformations and consequently, the strains are transferred from the panel zone to the inside of the beam beyond the constructed region of the connection. Lateral torsional buckling of the beam occurs as a result of beam flange yielding in the region beyond the cover plates, and subsequently, local buckling of the flange and web of the beam takes place. In such statuses, the obtained hysteresis curves become rectangular in shape and consequently, higher energy is absorbed by the connection with the increasing strength of the panel zone.

7.2. The effects of doubler and continuity plates

The rib and channel connections have been subjected to cyclic loading. Table 7 shows the results, including the energy dissipated by sub-assemblage, maximum rotation of the panel zone and the energy dissipated by the panel zone. The columns 4 and 5 of this table present the percentage of dissipated energy and panel zone rotation regarding the connection without continuity and doubler plates. According to the third column of the table, the energy that results due to the plasticity is slightly absorbed by the panel zone in the absence of continuity or doubler plates. This absorbed energy is little compared to the entire energy and shows that the panel zone has lost its elastic status. However, in cases where the continuity and doubler plates are used together, the amount of energy is zero, indicating the appropriate performance of the panel zone during the seismic loading.

In the rib connection, higher energy was absorbed in the RIB TD8C sample (68%), whereas the panel zone rotation shows 91% reduction. The energy absorbed in RIB TD15C sample is 81%, 13-15% higher than that of RIB TD8C; the panel zone rotation has been reduced by 1-2%.

Table 7: The results of constructed connection

Models	Dissipated energy (kJ)	Maximum panel zone rotation (×10⁻³)	Energy of panel zone (kJ)	Dissipated energy (%)	Panel zone rotation (%)
RIB TD0	51202	17.7102	6.16	0	0
RIB TD0C	61298	8.6518	4.80	19.72	-51.15
RIB TD8	63163	4.0892	0.66	23.36	-76.91
RIB TD8C	86152	1.4713	0	68.26	-91.69
RIB TD15	72167	2.7324	0.28	40.95	-84.57
RIB D15C	93047	1.2497	0	81.73	-92.94
CH TD0	60535	14.0039	5.85	0	0
CH TD0C	65478	7.8634	4.31	8.17	-43.85
CH TD8	69950	3.2553	0.46	15.55	-76.75
CH TD8C	83591	1.4482	0	38.09	-89.66
CH TD15	78171	2.2751	0.19	29.13	-83.75
CH TD15C	87216	1.2386	0	44.08	-91.16

In the channel connection, the energy that was absorbed in CH TD8C sample was 38% higher than that of CH TD0; while the panel zone rotation shows 89% reduction. The energy absorbed by CH TD15C sample is 44%, increasing by 6-7% in comparison to that of CH TD8C; the panel zone rotation was reduced by 1-2%.

With respect to these values, it was concluded that the amount of energy absorbed by the channel connection is lower than that of rib considering the effect of panel zone thickness. The results related to the energy absorbed by the suggested connection come close to each other with changing thickness of panel zone from half thickness of the web into the column web thickness in the presence of continuity plates.

It was observed that increasing the stiffness of the panel zone and adding the continuity and doubler plates would result in significant increase of absorbed energy and decrease of panel zone rotation.

The effects of panel zone thickness and presence of continuity plates are reduced in the connection models with simultaneous use of these plates. In such cases, the results are very close to each other. The presence or absence of continuity plates affects the results more significantly compared to that of doubler plates.

7.3. Truss point location

Shear yielding is initiated at the first point with maximum shear stress along the centerline of the beam beyond the connection reinforcement region. This point is called truss point (Arlekar and Murty, 2004 [3]). Fig. 10 shows the distribution of shear stress (τ_{xz}) along the neutral axis of the beam for connections constructed with channels of different panel zones. The distance of truss point from the end of connection reinforcement region is called the length (l_t) of

truss for 4.00% drift level, listed in Table 8. According to the third column of this table, the ratio of the length (l_t) of truss to beam depth is almost 0.5. Therefore, the assumption considered in the connection design is accurate.

Table 8: Truss point location

Models	Truss point distance from column face (mm)	l_t (mm)	l_t/d_b
CH TD0	279	124	0.4
CH TD0C	294.5	139.5	0.45
CH TD8	294.5	139.5	0.45
CH TD8C	310	155	0.5
CH TD15	294.5	139.5	0.45
CH TD15C	406.5	251.5	0.81
Average	313.18	158.18	0.51

Figs. 11-12 present Von Mises stress and equivalent plastic strain (output variable PEEQ in ABAQUS software) contours, respectively, in the joint region for different column panel zones at the end of the cyclic loading. The equivalent plastic strain in a material (PEEQ) is a scalar variable that is used to represent the material's inelastic deformation (Hibbitt *et al.*, 2011).

Based on Figs. 11-12, high stress and plastic strain are formed in the panel zone in the connection region of cover plates and ribs to the column, in the absence of continuity plates. During the analysis of specimen of weak column panel zone without continuity plates, the first yield sign is observed in the panel zone and beam flange beyond the reinforced region of connection simultaneously. Moreover, at the end of the loading, maximum plastic strain is formed in the panel zone. However, concerning other specimens, the first yield sign is seen in the beam flange beyond the reinforced region of the connection. This yield is followed by local buckling of beam flanges.
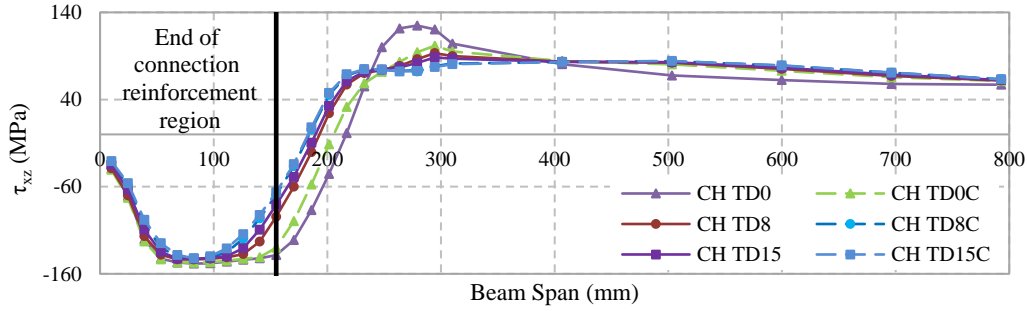
Fig. 10: Variation of shear stress (τ_{xz}) along beam centerline for different column panel zones

(a) CH TD0

(c) CH TD8

(e) CH TD15

(b) CH TD0C
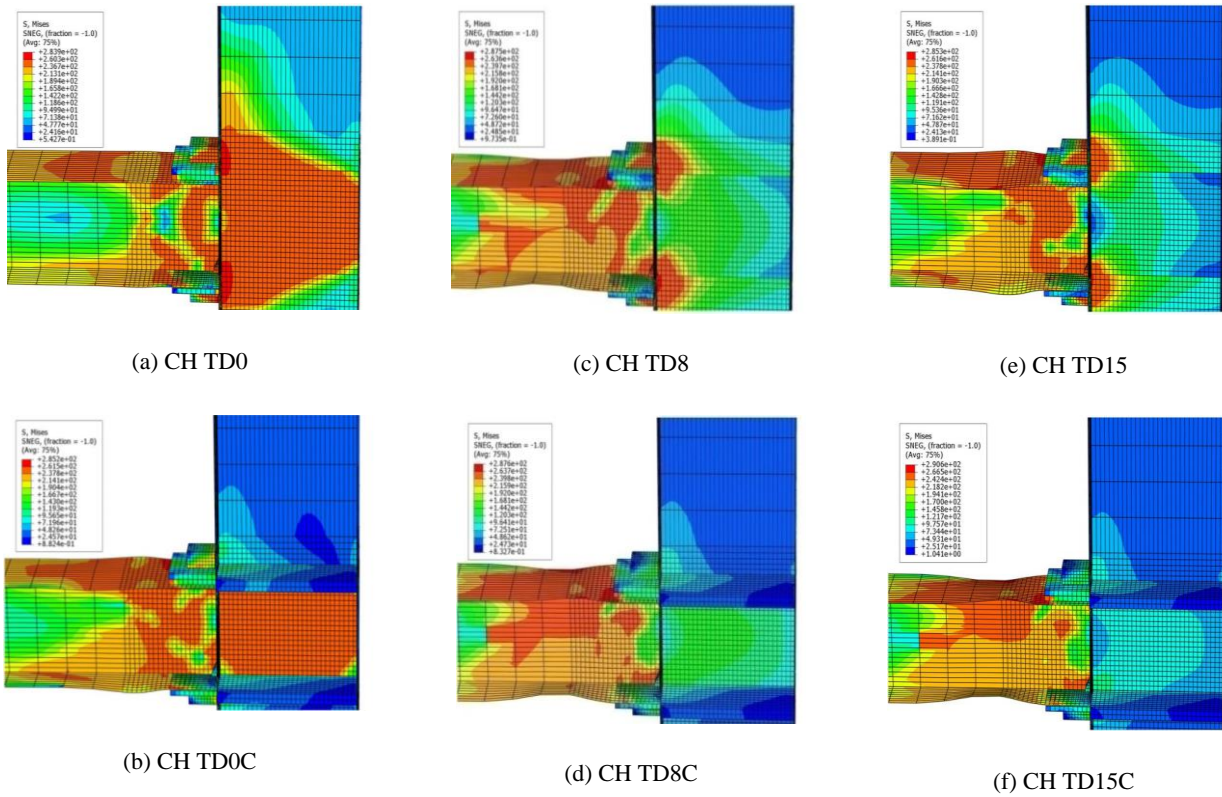
(d) CH TD8C

(f) CH TD15C

Fig. 11: Von Mises stress contours (MPa) of channel connection in the connection region for different panel zones at the end of the cyclic loading

Table 9: The results with changing the lengths of cover plates

Model	Dissipated energy (kJ)	Maximum panel zone rotation ($\times 10^{-3}$)	Dissipated energy (%)	Panel zone rotation (%)
RIB Cp0.5d_b	86152	1.4713	0	0
RIB Cp0.75d_b	92231	1.4970	7.06	1.75
RIB Cpd_b	98619	1.5550	14.47	5.69
CH Cp0.5d_b	83591	1.4480	0	0
CH Cp0.75d_b	97825	1.4650	17.03	1.17
CH Cpd_b	109819	1.5180	31.38	4.83

<div align="center">(a) CH TD0</div>

<div align="center">(c) CH TD8</div>

<div align="center">(e) CH TD15</div>

<div align="center">(b) CH TD0C</div>

<div align="center">(d) CH TD8C</div>
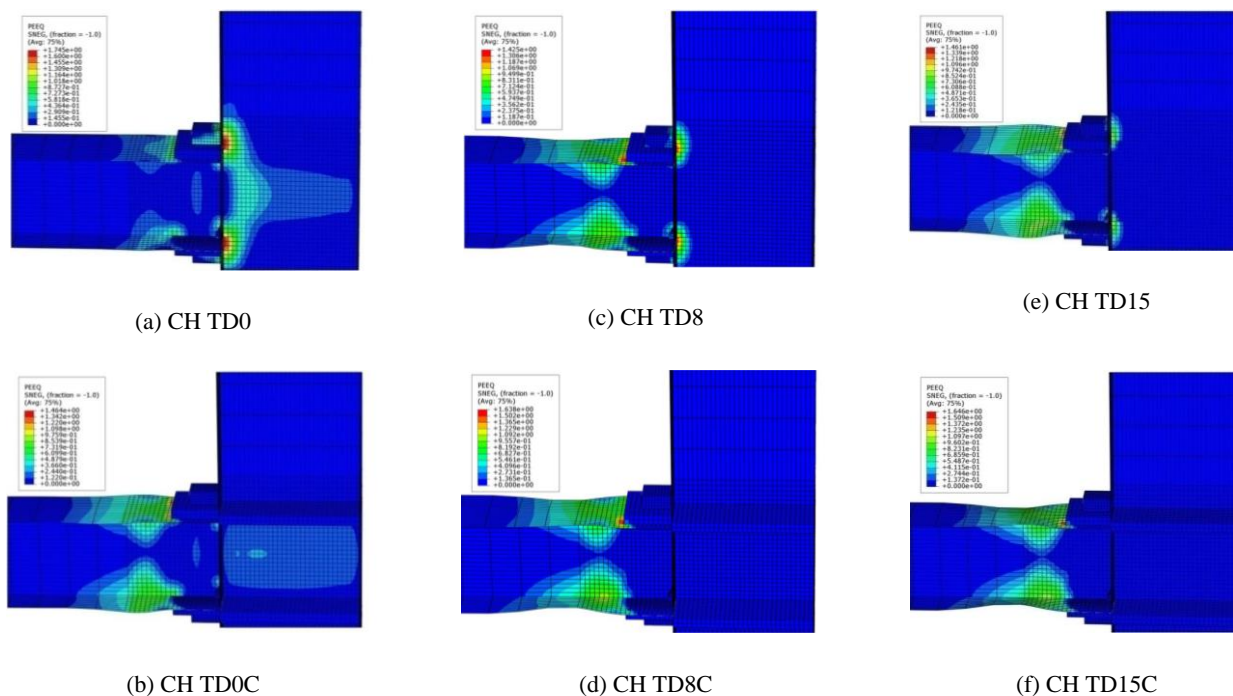
<div align="center">(f) CH TD15C</div>

Fig. 12: Equivalent Plastic Strain (PEEQ) contours of channel connection in the connection region for different panel zones at the end of the cyclic loading

7.4. Comparing the rib and channel connections

Fig. 13 shows maximum rotation of panel zone in the rib and channel connections concerning different statuses of panel zone. According to this figure and the results presented in Table 7, if the panel zone is without doubler or continuity plates, the rotation of panel zone is different in the rib and channel connections. This difference is reduced by adding the continuity plates to the panel zone. The rotation is slightly higher in the rib connection in all cases. Fig. 14 shows the energy dissipated by the previous and suggested connections. According to this figure, a slight difference is seen between the energy dissipated by rib and channel connections. However, in all cases without continuity plates in the panel zone, in the absence of doubler plates and presence of continuity plates, higher energy is absorbed by channel connection compared to rib connection.

The energy absorbed by rib connection is slightly higher in comparison to that of channel connection considering the addition of continuity and doubler plates to the panel zone.

7.5. The effects of cover plate length

Table 9 presents the results related to the changed cover plates' lengths in both rib and channel connections. The amount of energy dissipated by the connection and panel zone rotation increased with increasing lengths of cover plates compared to the case of using the cover plates with the length of half height of the beam. In the case of increasing the cover plates' lengths to 75% of beam height in the rib connection, the absorbed energy is 7-8%, whereas in channel connection it is 17-18%. This fact indicates that the channel connection is significantly affected by the lengths of cover plates in comparison to that of rib.

According to Figs. 15-16, the absorbed energy and panel zone rotation are slightly different in the two kinds of connections regarding different cover plates' lengths. As expected, the plastic hinge is formed in the beam beyond the strengthened region of the connection in all specimens. Therefore, the suggested connection shows more appropriate performance in seismic loading.
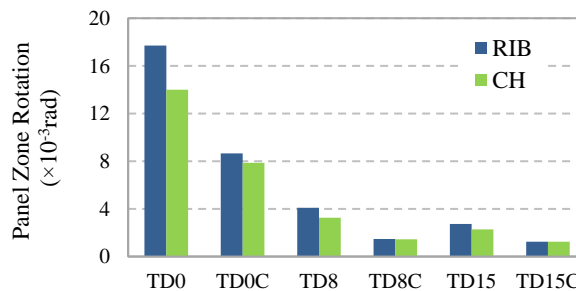

Fig. 13: Comparing the panel zone rotation in rib and channel connections
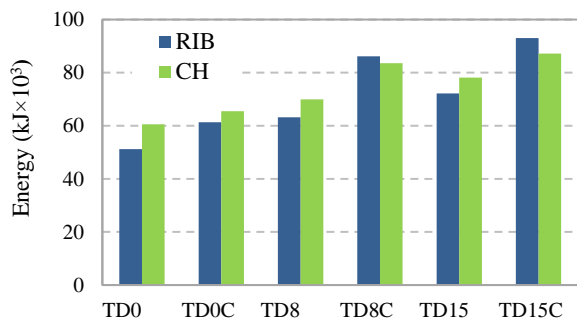
Fig. 14: Comparing the dissipated energy of rib and channel connections
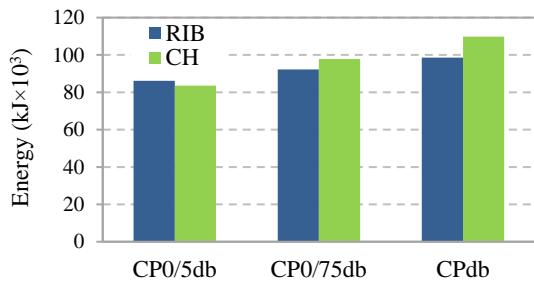

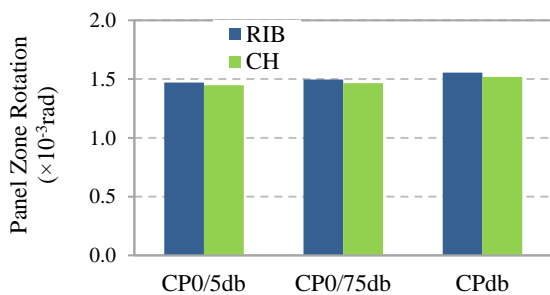**Fig. 15:** The dissipated energy with respecting to the different lengths of cover plates

Fig. 16: Panel zone rotation in rib and channel connections for different cover plate length

8. Conclusion

In conclusion, this study focuses on the seismic performance of the channel connection. The connection was designed by truss analogy model. The effects of the cover plates' length, panel zone thickness and the presence of continuity plates have also been assessed. The obtained results were compared with those of rib connections. However, cyclic strength degradation and fracture which could have a significant effect on the response of the connection, are not modelled.

Compared to the rib connections, a distinctive specification of the suggested connection is that the suggested connection does not have the limitation of ribs (e.g. rotation during welding and adjusting it for welding) in the implementation due to the channel symmetry compared to the rib connections. Channel connection is easily implemented by two weld beads.

The following results have been obtained from finite element analyses:

If the panel zone has sufficient strength, the channel connection will support 0.06 rad drift without any significant strength reduction. Therefore, it can be presented as an implementable connection in special moment resistant frames.

The results of the suggested connection are slightly different from that of rib connection in the case of changing the lengths of covers plates. As a matter of fact, the rotation of panel zone is similar in the specimens with ribs and channels. However, the energy dissipated by the connection with channel is higher comparing to that of connection with ribs. Besides, the presented connection is more appropriate due to its uncomplicated implementation.

In the statuses of panel zone without continuity plates, higher energy is absorbed by the channel connection compared to rib connection. Besides, maximum rotation of the panel zone is lower in the proposed connection in comparison to rib connection.

If the panel zone has insufficient strength (weak panel zone) and no continuity plates are used, high rotation is created in the panel zone in both connections and great plastic strain is formed in the panel zone.

In the cases where the continuity or doubler plates are not used, insignificant energy is obtained because of plasticity which indicates the formation of plastic strain in the panel zone and its improper performance.

9. References

[1] American Institute of Steel Construction (AISC). (2010). ''Seismic Provisions for Structural Steel Buildings.'' Chicago.

[2] American Institute of Steel Construction (AISC). (2010). ''Specification for Structural Steel Buildings.'' Chicago.

[3] Arlekar, J .N., Murty, C. V. R. (2004). ''Improved Truss Model for Design of Welded Steel Moment-Resisting Frame Connections.'' J. Struct. Eng., 130(3), 498-510.

[4] Chen, C. C., Chen, S. W., Chung, M. D, Lin, M. C. (2004). ''Cyclic behavior of unreinforced and rib-reinforced moment connections.'' Journal of Constructional Steel Research, 61, 1–21.

[5] Chen, C.C., Lin, C.C., Tsai, C. L. (2004). ''Evaluation of reinforced connections between steel beams and box columns.'' Engineering Structures, 26, 1889–1904.

[6] Chen, C.C., Lu, C.A., Lin, C.C. (2005). ''Parametric study and design of rib-reinforced steel moment connections.'' Engineering Structures, 27, 699–708.

[7] Federal Emergency Management Agency (FEMA). (2000). ''Recommended seismic design criteria for new steel moment-frame buildings.'' FEMA 350, SAC Joint Venture, Calif.

[8] Federal Emergency Management Agency (FEMA). (2000). ''State of the Art Report on Connection Performance.'' FEMA 355d, SAC Joint Venture, Calif.

[9] Goel, S. C., Stojadinovic, B. and Lee, H. K. (1996). ''A new look at steel moment connections.'' Rep. No. UMCEE 96-19, Univ. of Michigan College of Engineering.

[10] Goel, S. C., Stojadinovic, B., Lee, H. K. (1997). ''Truss Analogy for Steel Moment Connections.'' Eng. J., Second Quarter, 43–53.

[11] Goel, S.C., Lee, K.H., Stojadinovic, B. (2000). ''Design of Welded Steel Moment Connections Using Truss Analogy.'' Eng. J., First Quarter, University of Utah Interlibrary Loan.

[12] Goswami, R., Murty, C. V. R. (2010). ''Externally Reinforced Welded I-Beam-to-Box-Column Seismic Connection.'' J. Eng. Mech., 136(1), 23-30.

[13] Hibbitt, D., Karlsson, B., Sorensen, P. (2011). Simulia ABAQUS 6 .11 Users' Manual.

[14] Lee, C. H. (2005). ''Review of force transfer mechanism of welded steel moment connections.'' Journal of Constructional Steel Research, 62, 695–705.

[15] Lee, K. H.,Goel, S. C.,Stojadiovic, B. (1998). ''Boundary Effects in Welded Steel Moment Connections.'' Proc., 6th U.S. National Conf. on Earthquake Engineering.

[16] Lee, K.H.,Goel, S. C.,Stojadinovic, B. (2000). ''Boundary Effects in Steel Moment Connections.'' Paper No. 1098, Proc., 12th World Conf. on Earthquake Engineering, Auckland, New Zealand.

[17] Lee, C. H., Jung, J. H., Oh, M. H., Koo, E. S. (2005). ''Experimental Study of Cyclic Seismic Behavior of Steel Moment Connections Reinforced with Ribs.'' Journal of Structural Engineering, 131(1), 108-118.

[18] Mahin, S.,Malley, J., Hamburger R. (2002). ''Overview of the FEMA/SAC Program for Reduction of Earthquake Hazards in Steel Moment Frame Structures.'' Journal of Constructional Steel Research, 58, 511–528, 2002.

[19] Miller, D.K. (1998). ''Lessons Learned from the Northridge Earthquake.'' Eng. Struct., 20(4-6), 249-260.

[20] Tremblay, R., Timler, P., Bruneau, M., Filiatrault, A. (1995). ''Performance of steel structures during the 1994 Northridge earthquake.'' Can. J. Civ. Eng., 22, 338-360.